Journal of Materials Processing Technology 177 (2006) 150–153

Journal of Materials Processing Technology

www.elsevier.com/locate/jmatprotec

Investigation of a slab method analysis and FEM simulation on rotating compression forming of ring

Gow-Yi Tzou [a], Hung-Hsiou Hsu [b,*], Yun-Hsiu Hsiao [a]

[a] *Department of Mechanical Engineering, Yung-Ta Institute of Technology, Pingtung 909, Taiwan, ROC*

[b] *Department of Management Information Science, Institute of Health Information Management, Chia-Nan University of Pharmacy & Science, Tainan 717, Taiwan, ROC*

Abstract

An investigation into the compression forming of a billet using the commercial code SUPERFORM is developed. The work-piece of the ring billet compressed between the upper and lower dies is meshed by a hexagon rigid-plastic element. The numerical simulation based on the FEM is also compared to results obtained with the slab method. In the slab method analysis, the stress distribution of the work-piece is estimated assuming coulomb friction between the dies and the work-piece. The effects of frictional coefficient, rotating angular speed, reduction and aspect ratio upon the compression force, the effective stress and the effective strain, are discussed. For verifying the validity of these models, an aluminum alloy A6061 ring billet is examined in the experiment of rotating compression forming of ring. The analytical results provide a good agreement with the experiment and useful knowledge of design of the compression forming of ring billet.

Keywords: Rotating compression forming; FEM; Slab method

1. Introduction

The compression test of a cylinder is used for determining the frictional coefficient and the mechanical strength of billet material, the compression load, the stress on the die, the heat transfer between billet and room temperature. It can provide useful data for the die design and production design in metal forming process. Lee and Altan [1] used the upper bound method to propose a kinematically admissible velocity field for investigating the flow stress and frictional coefficient in the ring and cylinder compression process. Xue et al. [2] used the finite element method to explore the plastic deformation of cylinder billet in the twist compression forming process. It indicates that the compression force and geometric profile of deformed billet were reduced. Kim et al. [3] utilized the dual stream function to explore plastic behaviors as the tool is rotating but the cylinder is not. Chien et al. [4] have first established the theoretical analysis to discuss the rotating compression of ring based on the slab method. Hsu et al. [5] proposed a numerical simulation on rotating compression forming of ring based on finite element method. It also considers constant frictional factor to explore the compression force by using the slab method with constant sheer friction. The effects of frictional factor, rotating angular velocity, reduction, aspect ratio, etc. upon compression force, effective stress distribution, effective strain distributions and velocity field are obtained by FEM. However this study considering constant frictional coefficient for coulomb friction is proposed to determine the compression characteristics based on the FEM, and to compare to the slab method and experiment.

2. FEM simulation

In this paper, the rotating compression of the ring is simulated by using the commercial software package—SUPERFORM. It can provide the elastic–plastic and rigid-plastic simulation of the metal forming in large deformation, and permits tool design and product design. It also provides hexagonal and tetrahedral elements for meshing the work-piece of bulk forming and the auto re-mesh step is enveloped in the software package. Using SUPERFORM, it can significantly reduce the cost and time consumption of tool and die design.

The flow pattern, equivalent stress distribution, equivalent strain distribution, velocity field of work-piece and load stoke

* Corresponding author.
E-mail addresses: tzougowyi@yahoo.com.tw (G.-Y. Tzou), hhhsu127@mail.chna.edu.tw (H.-H. Hsu), asdwiner@yahoo.com.tw (Y.-H. Hsiao).

0924-0136/$ – see front matter © 2006 Elsevier B.V. All rights reserved.
doi:10.1016/j.jmatprotec.2006.04.073

can be simulated by FEM. Such simulation results can be used to obtain the product geometric profile and material properties required.

In the preprocess of modelling the rotating compression forming, the 3D mechanical type, the geometric profile of ring, the contacted surface by using GUI interface of the SUPERFORM are constructed. The elastic–plastic model is chosen and the material properties, such as Young's modulus, Poisson's ratio, density, are needed. The isotropic work hardening rule is assumed in flow rule due to plastic strain hardening. The change of the von Mises yield surface is plotted. The initial conditions of work-piece are set up, and the contact along work-piece and dies are defined. The load case is defined for the forming process and stage.

In rotating compression forming, the relationship between strain and stress is nonlinear. The SUPERFORM has been developed to resolve the nonlinear problem. Three aspects of nonlinear effects such as material nonlinearities, geometric nonlinearities, nonlinear boundary conditions are simulated. The conventional von Mises yield surfaces is available in SUPERFORM. The updated Lagrangian formulation can be used for solving geometrically nonlinear problems. The contact body can be chosen as deformable bodies or a deformable-body and a rigid surface, and the nonlinear boundary conditions can be solved. In solving nonlinear problem, the governing equation must be solved incrementally as the following:

$$K\,\mathrm{d}\mathbf{u} = \mathrm{d}\mathbf{f} \tag{1}$$

where d**u** and d**f** are the increments of displacement and force vectors.

The convergence of the nonlinear system for the SUPERFORM is evaluated by examining either stress residuals or displacements. The default statement for the convergence is satisfied under any of the foregoing convergent criteria.

3. Slab method analysis

Fig. 1 shows the schematic diagram of rotating compression forming of the ring. Assuming the neutral point is happened between the inner radius and the outer radius. Fig. 2 shows the schematic diagram of a small element of the ring in Zones I and II, where ω is the angular speed of the lower die, and ρ the material density of the ring. For deriving the analytical model of the rotating ring compression, the following assumptions are employed:

(1) The ring compressed is a rigid-plastic material.
(2) Axi-symmetrical compression is assumed, thus the radial stress (σ_r) equals the circumferential stress (σ_θ).
(3) The stresses distributed within the elements are uniform. The radial stress (σ_r), the circumferential stress (σ_θ), and the vertical stress (σ_z) are regarded as principal stresses.
(4) The friction between the dies and the ring are assumed to be constant shear friction ($\tau = \mu p$), and it acts on a certain orientation relative to the r-axis (i.e. the α angle).

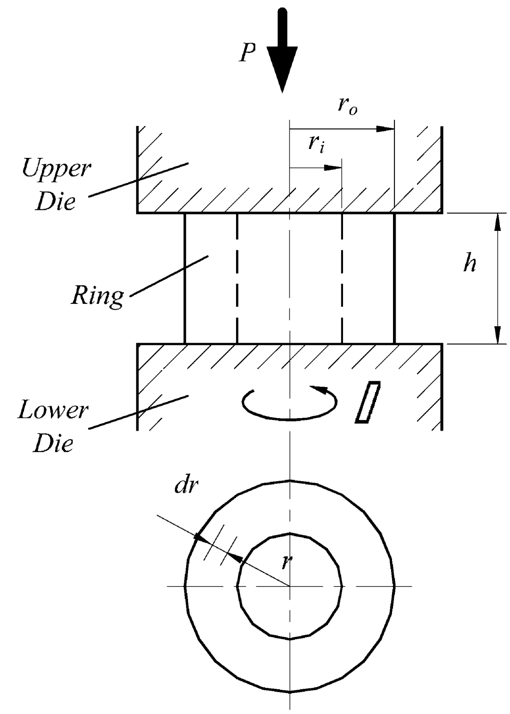

Fig. 1. Schematic diagram of rotating compression forming of the ring.

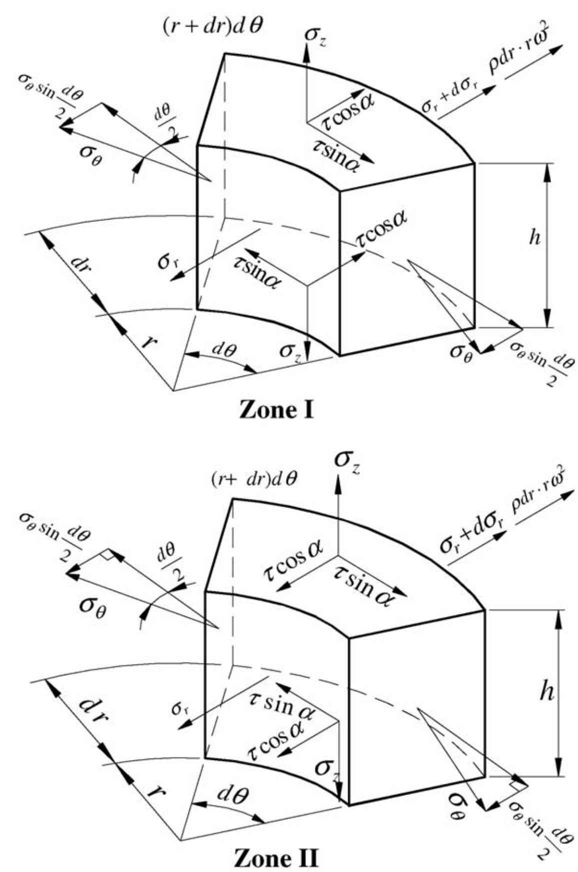

Fig. 2. Schematic diagram of a small element of the ring in Zones I and II.

3.1. Compression pressure

Force equilibrium equations, yield criteria, geometrical conditions, boundary conditions, and frictional conditions, are used to derive the compression characteristics such as the compression pressure distribution, the radial stress distribution and the compression force. First of all, the horizontal force equilibrium equation in Zones I and II are derived.

- Zone I ($r_i \le r \le r_n$):

$$\frac{d\sigma_r}{dr} + \rho r\omega^2 = -\frac{2\tau\cos\alpha}{h} \quad (2)$$

- Zone II ($r_n \le r \le r_0$):

$$\frac{d\sigma_r}{dr} + \rho r\omega^2 = \frac{2\tau\cos\alpha}{h} \quad (3)$$

The foregoing equations are the governing equations in the rotating compression forming of the ring, where $\tau = \mu p$.

The yield criteria are used as follows:

$$\sigma_r - \sigma_z = Y = \begin{cases} \sqrt{3}k \text{ (von Mises)} \\ 2k \text{ (Tresca)} \end{cases} \quad (4)$$

Let $\sigma_r = q$ and $\sigma_z = -p$ substitute into Eq. (4), then getting:

$$p + q = Y \quad (5)$$

Combining Eq. (5) with Eqs. (2) and (3), Eqs. (2) and (3) become:

$$\frac{dp}{dr} - \frac{2\tau\cos\alpha}{h} = r\rho\omega^2, \quad \text{for zone I} \quad (6)$$

$$\frac{dp}{dr} + \frac{2\tau\cos\alpha}{h} = r\rho\omega^2, \quad \text{for zone II} \quad (7)$$

The governing equations can be solved to obtain the compression pressure, p, respectively:

$$p_{\mathrm{I}} = c_1\,e^{rB} - \frac{\rho\omega^2}{B}\left(r + \frac{1}{B}\right) \quad (8)$$

$$p_{\mathrm{II}} = c_2\,e^{-rB} + \frac{\rho\omega^2}{B}\left(r - \frac{1}{B}\right) \quad (9)$$

where $B = (2\mu\cos\alpha)/h$ and c_1 and c_2 are integral constants determined by the boundary conditions.

Boundary conditions:

- Zone I ($r_i \le r \le r_n$):
  At $r = r_i$, $q = 0$, $p = Y$; c_1 is obtained as

$$c_1 = Y\,e^{-r_iB} + \frac{\rho\omega^2}{B}e^{-r_iB}\left(r_i + \frac{1}{B}\right) \quad (10)$$

- Zone II ($r_n \le r \le r_0$):
  At $r = r_0$, $q = 0$, $p = Y$; c_2 is obtained as

$$c_2 = Y\,e^{r_0B} - \frac{\rho\omega^2}{B}e^{r_0B}\left(r_0 - \frac{1}{B}\right) \quad (11)$$

According to the yield criteria, the radial stress distribution (q/Y) can be also expressed as

$$\frac{q}{Y} = 1 - \frac{p}{Y} \quad (12)$$

The specific compression pressures in two zones can be arranged as follows:

$$\left(\frac{p}{Y}\right)_{\mathrm{I}} = e^{B(r-r_i)} + \frac{\rho\omega^2}{BY}e^{B(r-r_i)}\left(r_i + \frac{1}{B}\right) - \frac{\rho\omega^2}{BY}\left(r + \frac{1}{B}\right) \quad (13)$$

$$\left(\frac{p}{Y}\right)_{\mathrm{II}} = e^{B(r_0-r)} - \frac{\rho\omega^2}{BY}e^{B(r_0-r)}\left(r_0 - \frac{1}{B}\right) + \frac{\rho\omega^2}{BY}\left(r - \frac{1}{B}\right) \quad (14)$$

3.2. Determination of the neutral point

The compression pressures at the neutral point (r_n) remain continuous, so at $r = r_n$, $p_{\mathrm{I}} = p_{\mathrm{II}}$; the neutral point can be found:

$$c_1\,e^{r_nB} - c_2\,e^{-r_nB} - \frac{2r_n\rho\omega^2}{B} = 0 \quad (15)$$

3.3. Compression force

The compression force can be expressed as

$$P = P_{\mathrm{I}} + P_{\mathrm{II}} \quad (16)$$

4. Experimental

In this research, the specimens of billet are the rings with the dimension $d_0 \times d_i = 24\,\mathrm{mm} \times 12\,\mathrm{mm}$, the initial heights of specimen are divided as four group of $h_i = 8$, 12, 24 and 36 mm, respectively. The standard specimen dimension of 6:3:2 ring specimen is $d_0 \times d_i \times h_i = 24\,\mathrm{mm} \times 12\,\mathrm{mm} \times 8\,\mathrm{mm}$. Aluminum alloy A6061 is used to be the test material.

The schemes of rotating compression forming experiment of the ring are as follows:

(1) The angular velocity with rotation is $\omega = 0.16$ rad/s and no rotation, $\omega = 0$, respectively.
(2) The compression forces of rotating compression forming of the ring are measured.
(3) The geometries of the deformed rings are measured.
(4) Variations of the compression force with reduction are explored.

5. Results and discussions

Fig. 3 shows the effect of rotating angular speed upon the ring shape deformed under the different reductions. At each reduction, the bugling effect with rotation is smaller than that without rotation.

Figs. 4 and 5 show the comparisons of compression force among the slab method analysis, the FEM simulation, and the experiment, considering whether the rotation is considered or not. The conditions are $\omega = 0$, $\omega = 0.16$ rad/s, and $\mu = 0.214$. The analytical values by the slab method and the FEM simulation are both close to the experimental data. Most results from the

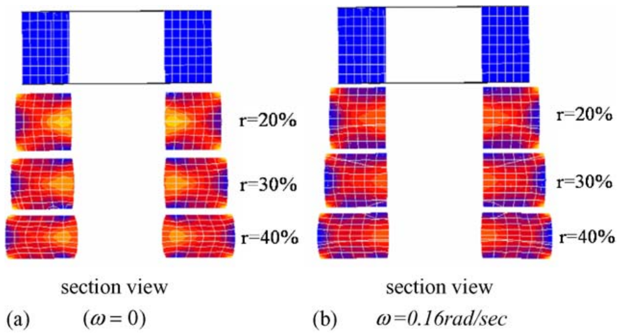

Fig. 3. Effect of rotating angular speed upon the ring shape deformed under the different reductions ($h_i = 8$ mm, $\mu = 0.15$).

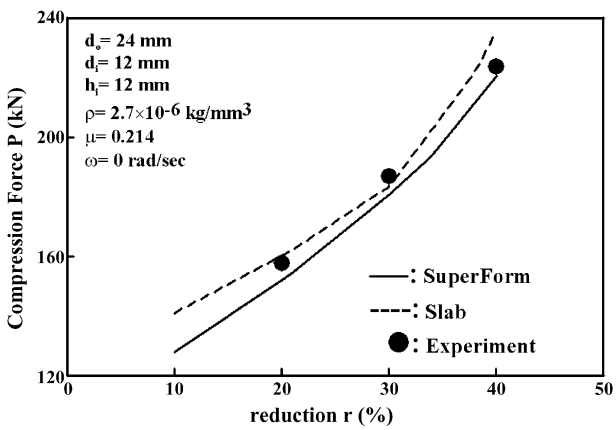

Fig. 4. Comparisons of compression force among the slab method analysis, the FEM simulation, and the experiment.

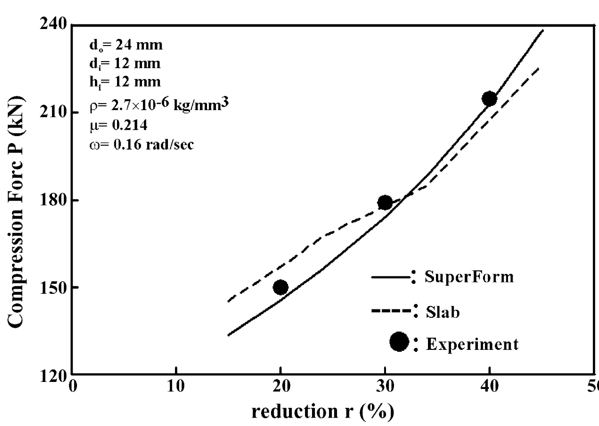

Fig. 5. Comparisons of compression force among the slab method analysis, the FEM simulation, and the experiment.

SUPERFORM are in closer agreement with the experiment than those of the slab method. It is helpful to understand the compression forming of Aluminum alloy A6061.

6. Conclusion

The conclusions can be summarised as follows:

(1) By FEM simulation, the inner and outer shapes can be predicted, and the compression force is more precise than the slab method in comparison to experiment.
(2) The compression force increases with decreasing initial height of ring at fixed reduction in height.
(3) The rotating angular velocity (ω) can effectively reduce the equivalent strain and stress. The compression force varies less as the rotating angular velocity increases.
(4) The rotating angular velocity (ω) can effectively reduce the bulging effect and the section of ring remains closer to a rectangle.

Acknowledgements

This work was sponsored by the National Science Council of Republic of China under grant No. NSC-92-2212-E-132-003. The advice and financial support of the NSC are gratefully acknowledged.

References

[1] C.H. Lee, T. Altan, Influence of flow stress and friction upon metal flow in upset forging of ring and cylinders, J. Eng. Ind. (1972) 775–781.
[2] K.M. Xue, Z. Wang, Y. Lu, FEM analysis of cylinder twist compression deformation regularity, J. Mater. Process. Technol. 69 (1997) 148–151.
[3] Y.H. Kim, Y.E. Jin, J.H. Park, Y. Lee, An analysis of the torsional forming process using the dual stream function, in: M. Pietrzyk, J. Kusiak, J. Majta, P. Hartley, I. Pillinger (Eds.), Proceedings of the Eight International Conference on Metal Forming, Publ. A. Balkema, Krakow, 2000, pp. 741–745.
[4] W.T. Chien, G.Y. Tzou, M.N. Huang, W.H. Tseng, Theoretical analysis of rotating compression forming of ring considering constant shear friction, J. Steel Relat. Mater.—Steel Grips Suppl. Metal Forming 2004 (2004) 671–675.
[5] H.H. Hsu, G.Y. Tzou, W.T. Chien, W.H. Tseng, Study on rotating compression forming of ring based on the finite element method and experiment, J. Chin. Soc. Mech. Eng. 26 (2005) 485–491.